genes encoded transmembrane proteins, and 6, 8 and 7 genes encoded secreted proteins from LNCaP, DU145 and normal prostate CAST libraries, respectively. Because the purpose of this study was to identify genes that encode transmembrane proteins present in PCa, we focused on transmembrane proteins.

Identification of Genes Expressed More Highly in PCa than in Normal Tissues

To identify genes expressed specifically in PCa, we compared the gene list from each PCa cell line CAST library to the normal prostate CAST library. We only selected genes that were detected at least twice in each PCa cell line CAST library. In addition, genes were selected that were not found in the normal prostate CAST library. We obtained 6 candidates from LNCaP and 14 candidates from DU145. In total, 18 individual candidate genes were identified (table 2). To confirm that these candidates were PCa specific, quantitative RT-PCR was performed to measure the expression of these candidates in 9 PCa and 15 normal tissue samples. Representative results are shown in figure 1. Expression of the 18 candidate genes was not necessarily specific for PCa. However, several genes showed much higher expression in PCa than in normal tissues. We then focused on cancer specificity by calculating the specificity index for each gene (table 2). Of the 18 candidates, STEAP1 was found to show a high specificity for PCa, and 2 genes, *ADAM9* and *CDON*, were found to show a low specificity for PCa. The expression levels of the 18 genes in PCa tissue samples were also compared to those in normal prostate tissue samples. As shown in table 2, overexpression (tumor/normal prostate tissue ratio >2) was observed for all 18 genes. Among the 9 PCa cases, corresponding nonneoplastic prostate tissue samples were available for quantitative RT-PCR from 5 cases. The expression levels of the 18 genes in 5 samples of corresponding nonneoplastic prostate tissue were analyzed by quantitative RT-PCR. Frequent overexpression (tumor/nonneoplastic prostate tissue ratio >2) was found for all 18 genes (data not shown).

Overexpression of *STEAP1* and *ADAM9* in PCa has been reported [17, 18]; however, expression of *CDON* in human cancers including PCa has not been investigated. Therefore, expression of *CDON* was analyzed by quantitative RT-PCR in an additional 6 PCa samples and corresponding nonneoplastic prostate samples. We calculated the ratio of *CDON* mRNA expression levels between PCa tissue (T) and corresponding nonneoplastic prostate (N). T-to-N ratios >2 were considered to represent overexpression. Among 6 cases, 5 (83%) cases showed *CDON* overexpression.

Table 2. Summary of quantitative RT-PCR analysis of candidate genes specifically expressed in PCa

Gene name	Normal organ with highest expression		PCa (B)[1]	Specificity index (B/A)	PCa case No.[2]
	organ	mRNA expression level (A)			
High specificity					
STEAP1	pancreas	7.51	93.5[†]	12.5	9
Low specificity					
ADAM9	prostate	1.0	6.8	6.8	5
CDON	skeletal muscle	11.1	24.9	2.2	9
No specificity					
CTCL	pancreas	4.2	8.1	1.9	7
DSC2	heart	4.8	6.7	1.4	8
TNFRSF10D	pancreas	30.7	31.1	1.0	4
DNAJB14	heart	4.3	3.7	0.9	4
DLG1	pancreas	7.7	6.1	0.8	3
ADAM17	pancreas	3.8	2.8	0.7	2
SLC30A9	heart	32.0	20.2	0.6	5
PTP4A1	skeletal muscle	30.0	18.2	0.6	5
SGCE	heart	17.2	9.3	0.5	2
TMEM161B	pancreas	11.2	5.9	0.5	4
STX4	heart	12.2	4.3	0.4	4
LYSMD3	skeletal muscle	9.3	3.1	0.3	1
TM9SF3	pancreas	78.8	23.4	0.3	4
ITGB1	heart	23.4	6.7	0.3	2
TFRC	heart	42.5	10.4	0.2	4

The units are arbitrary. Target mRNA expression levels were standardized to 1.0 μg total RNA from normal prostate as 1.0.
[1] With highest expression mRNA expression level.
[2] With mRNA expression level 2-fold greater than normal prostate. [†] Arbitrary.

Effect of CDON Inhibition on Cell Growth and Invasive Activity

CDO protein is thought to be a strong candidate to mediate some of the effects of cell-cell contact that are important in myogenesis; however, the function of *CDON* in human cancers including PCa has not been reported. We performed Western blot analysis in LNCaP and DU145 cell lines. High CDO protein expression was found in DU145 cells as a band of approximately 139 kDa, and LNCaP cells had low or no CDO protein expression (fig. 2a). In CAST analysis, colonies containing *CDON* gene were detected twice in the DU145 CAST library, whereas no colonies with this gene were detected in the LNCaP CAST library, indicating that Western blot analysis of CDO protein was consistent with CAST anal-

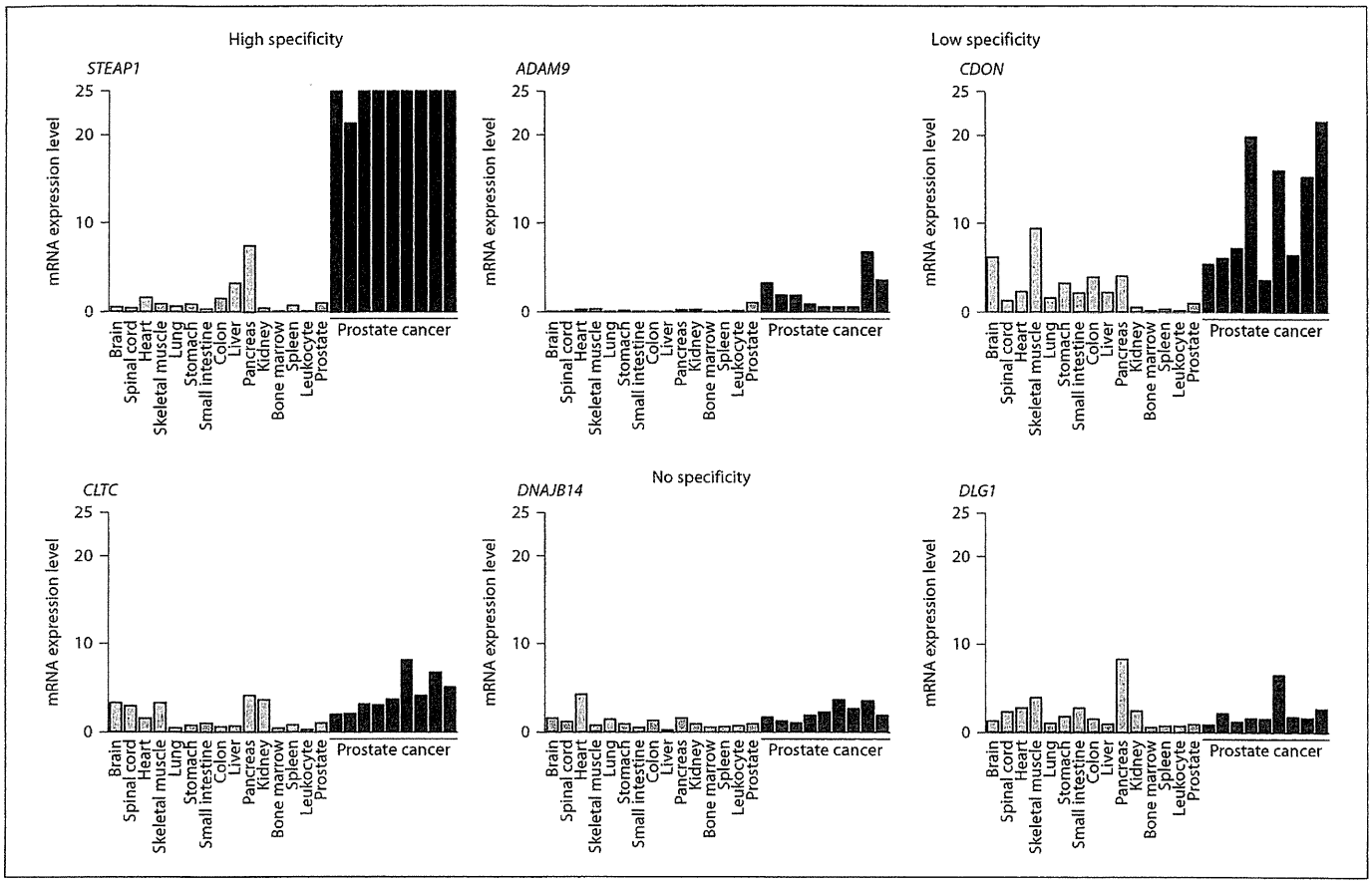

Fig. 1. Quantitative RT-PCR analysis of candidate genes that encode cell surface proteins in 15 normal tissues and 9 PCa samples. mRNA expression levels of *STEAP1*, *ADAM9* and *CDON* were much higher in PCa samples than in normal tissues. In contrast, mRNA expression levels of *CLTC*, *DNAJB14* and *DLG1* were not significantly different between PCa and normal tissues.

ysis. Next, we examined the transition of CDO protein expression by Western blot analysis of cell extracts of DU145 transfected with *CDON*-specific siRNAs. Three types of siRNAs (siRNA1–3) were transfected into DU145. The expression of CDO protein in DU145 was substantially suppressed by treatment with siRNA1, siRNA2 and siRNA3 (fig. 2b). We used siRNA1 in the following experiments to knock down the endogenous CDO protein. We also performed a time course analysis (from days 2 to 8) of *CDON* expression after siRNA transfection in DU145 cells. We confirmed suppression of *CDON* mRNA expression from days 2 to 8 after siRNA1 transfection by quantitative RT-PCR (data not shown).

To investigate the possible antiproliferative effect of *CDON* knockdown, we performed an MTT assay 8 days after siRNA transfection (fig. 2c). DU145 cells were selected for high CDO protein expression. *CDON* siRNA1-transfected DU145 cells showed significantly reduced viability relative to negative control siRNA-transfected DU145 cells. We performed the same assay using an LNCaP cell line that expressed low-level CDO protein. Reduced cell viability was not observed in siRNA1-transfected LNCaP cells compared with negative control siRNA-transfected LNCaP cells (fig. 2d). These results suggest that cell proliferation was activated or apoptosis was inhibited in *CDON* siRNA1-transfected DU145 cells. We examined the effect of *CDON* knockdown on the apoptotic susceptibility of DU145 cells to 5-FU. The frequency of apoptoitc cells in *CDON* siRNA1-transfected DU145 cells (mean, 71%) was significantly higher than that in negative control siRNA-transfected DU145 cells (mean 42%, $p = 0.0261$).

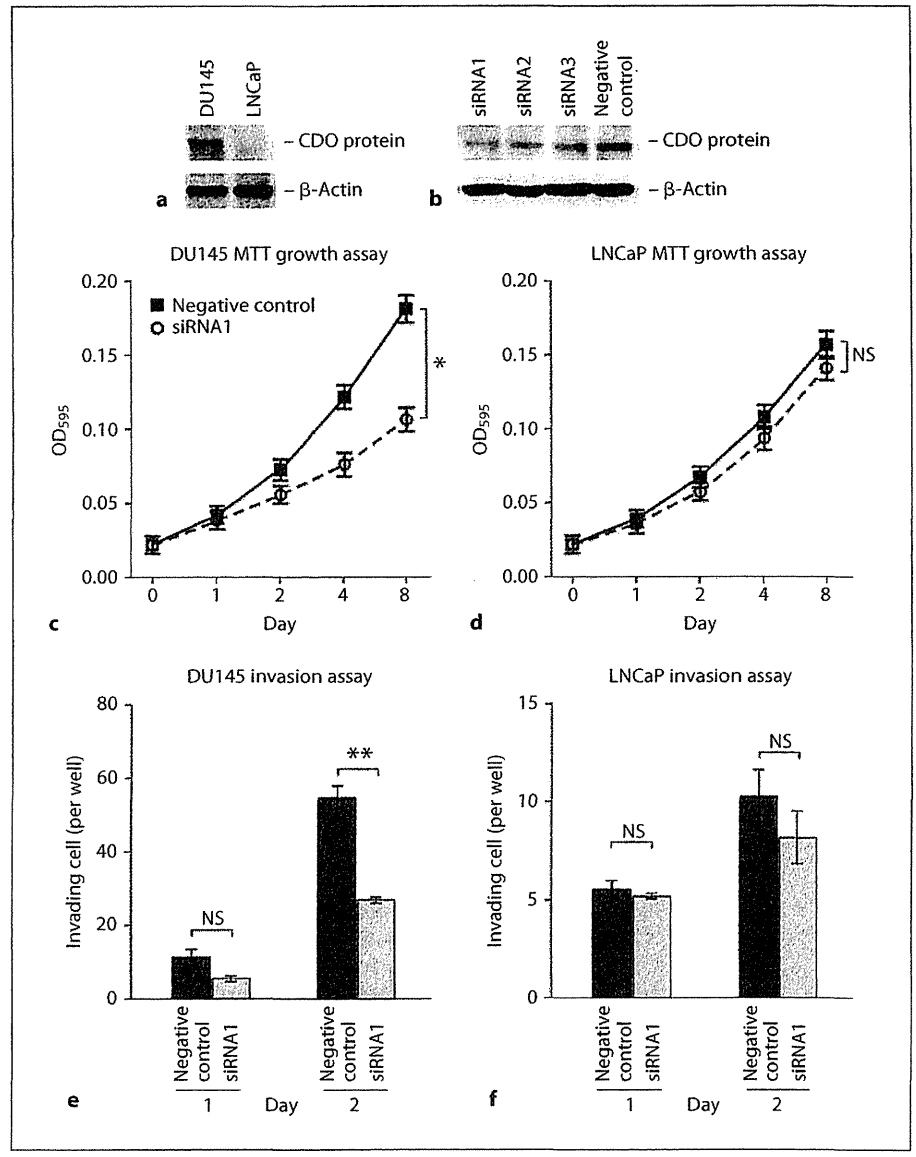

Fig. 2. CDO protein expression and functional analysis. Western blot analysis of CDO protein in PCa cell lines (**a**). Western blot analysis of CDO protein in DU145 cells transfected with the negative control siRNA and *CDON* siRNA (siRNA1–3) (**b**). Effect of *CDON* knockdown on cell growth of DU145 cells (**c**). Cell growth was assessed by an MTT assay at 1, 2, 4, and 8 days after seeding on 96-well plates in DU145 cells. Bars and error bars show means and SE of 3 different experiments. Effect of *CDON* knockdown on cell invasion of DU145 cells (**d**). After 1 and 2 days, invading cells were counted. Bars and error bars show means and SE of 3 different experiments. Cell growth was assessed by an MTT assay at 1, 2, 4 and 8 days after seeding on 96-well plates in LNCaP cells (**e**). Bars and error bars show means and SE of 3 different experiments. Effect of *CDON* knockdown on cell invasion of LNCaP cells (**f**). After 1 and 2 days, invading cells were counted. Bars and error bars show means and SE of 3 different experiments. NS = Not significant. * p = 0.0001; ** p = 0.0229.

Next, to determine the possible role of CDO protein in the invasiveness of PCa cells, we used a transwell invasion assay (fig. 2e). On day 2, although cell viability was not significantly different between *CDON* knockdown DU145 cells and negative control siRNA-transfected DU145 cells, the invasiveness of *CDON* knockdown DU145 cells was 50% less than that of the negative control siRNA-transfected DU145 cells. In contrast, invasion ability was not significantly different between *CDON* knockdown LNCaP cells and negative control siRNA-transfected LNCaP cells (fig. 2f). These results indicate that CDO protein stimulates invasion in PCa cells.

Discussion

We generated CAST libraries from 2 PCa cell lines, and identified several genes that encode transmembrane proteins present in PCa. Quantitative RT-PCR revealed that *STEAP1*, *ADAM9* and *CDON* were expressed much more highly in PCa than in 15 types of normal tissues. *STEAP1* showed the highest specificity for PCa. *STEAP1* encodes the STEAP-1 protein, which is a six-transmembrane cell surface protein. It has been reported that mouse monoclonal antibodies specific to STEAP-1 extracellular loops inhibit the growth of prostate and bladder tumor xenografts [17]. *ADAM9* showed the second highest spec-

ificity for PCa. ADAM proteins are zinc metalloproteases, which are involved in ectodomain shedding of growth factors, adhesion molecules, cytokines and receptors. ADAM9 has been shown to have proteolytic activity and its substrates include pro-HB-EGF, pro-EGF, the FGF receptor and so on [19, 20]. It has been reported that knockdown of *ADAM9* results in increased apoptosis and increased sensitivity to radiation in PCa cells [21]. These results indicate that both STEAP-1 and ADAM9 are therapeutic targets for PCa. In contrast, little is known about *CDON* expression in human cancers. In the present study, quantitative RT-PCR revealed that *CDON* was overexpressed in 83% of the PCa tissue samples, and knockdown of *CDON* in PCa cells induced 5-FU-induced apoptosis and inhibited invasion ability. These results suggest that *CDON* has the potential to constitute a therapeutic target for PCa.

The biological function of CDO protein is poorly understood. Previously, Kang et al. reported that CDO protein may have transformation suppressor function [10]. Expression of CDO protein was down-regulated in a rat embryo fibroblast cell line that was transformed by various oncogenes [10]. In addition, CDO protein levels were reduced when confluent cells were stimulated to re-enter the cell cycle. These results suggest that CDO protein may serve as a negative regulator of cell proliferation, transformation, and/or tumorigenesis. In the present study, knockdown of *CDON* in PCa cells induced 5-FU-induced apoptosis and inhibited invasion ability. Our present results are inconsistent with the previous reports, in which the function of CDO protein was investigated in rat embryo fibroblasts [10]. Here, we found that CDO protein in PCa cells may be different from fibroblasts.

On the other hand, it has been shown that the Sonic Hedgehog (SHh) directory interacts with CDO protein [22], and CDO protein functions to positively regulate SHh signaling in vivo and in vitro [23]. The Hh signaling pathway plays a central role during embryonic development and acts in stem cell renewal as well as tissue repair [24]. Hh ligands act via several components, including Patched and Smoothened transmembrane receptors, and lead to the activation of the Gli, a zinc-finger transcription factor. Several lines of evidence have indicated an association between Hh pathway activation and initiation or growth of several human cancers, including basal cell carcinomas, medulloblastomas and PCa [25, 26]. Therefore, it is possible that in addition to Patched, CDO protein also leads to the activation of the SHh pathway and participates in tumor cell growth in PCa.

Although *CDON* mRNA upregulation was observed in bulk PCa tissues by quantitative RT-PCR, expression and distribution of CDO protein in PCa tissues remains unclear. In this viewpoint, we performed immunohistochemical analysis in PCa tissue samples; however, obvious membranous staining was not found. The antibody against CDO protein used in the present study is not suitable for immunostaining because the antibody against CDO protein detected multiple bands on Western blots. Production of a specific antibody against CDO protein for immunostaining is required.

In summary, our present study yielded a list of genes that encode transmembrane proteins present in PCa. Our current data also provide information with respect to the expression of these genes throughout the body. We found that *CDON* is overexpressed in PCa, and *CDON* expression is narrowly restricted in normal tissues. Functional and immunohistochemical analysis will certify whether CDON may constitute a therapeutic target for PCa.

Acknowledgements

We thank Mr. Shinichi Norimura for his excellent technical assistance and advice. This work was carried out with the kind cooperation of the Research Center for Molecular Medicine, Faculty of Medicine, Hiroshima University. We thank the Analysis Center of Life Science, Hiroshima University, for the use of their facilities. This work was supported in part by Grants-in-Aid for Cancer Research from the Ministry of Education, Culture, Science, Sports and Technology of Japan.

References

1 Baade PD, Youlden DR, Krnjacki LJ: International epidemiology of prostate cancer: geographical distribution and secular trends. Mol Nutr Food Res 2009;53:171–184.

2 Carter HB: Prostate cancers in men with low PSA levels – must we find them? N Engl J Med 2004;350:2292–2294.

3 Chang SS, Kibel AS: The role of systemic cytotoxic therapy for prostate cancer. BJU Int 2009;103:8–17.

4 Isaacs W, De Marzo A, Nelson WG: Focus on prostate cancer. Cancer Cell 2002;2:113–116.

5 Buckhaults P, Rago C, St Croix B, et al: Secreted and cell surface genes expressed in benign and malignant colorectal tumors. Cancer Res 2001;61:6996–7001.

6 Ferguson DA, Muenster MR, Zang Q, et al: Selective identification of secreted and transmembrane breast cancer markers using *Escherichia coli* ampicillin secretion trap. Cancer Res 2005;65:8209–8217.

7 von Heijne G: A new method for predicting signal sequence cleavage sites. Nucleic Acids Res 1986;14:4683–4690.

8 Kadonaga JT, Gautier AE, Straus DR, Charles AD, Edge MD, Knowles JR: The role of the β-lactamase signal sequence in the secretion of proteins by *Escherichia coli*. J Biol Chem 1984;259:2149–2154.
9 Anami K, Oue N, Noguchi T et al: Search for transmembrane protein in gastric cancer by the *Escherichia coli* ampicillin secretion trap: expression of DSC2 in gastric cancer with intestinal phenotype. J Pathol 2010;221:275–284.
10 Kang JS, Gao M, Feinleib JL, Cotter PD, Guadagno SN, Krauss RS: CDO: an oncogene-, serum-, and anchorage-regulated member of the Ig/fibronectin type III repeat family. J Cell Biol 1997;138:203–213.
11 Kang JS, Mulieri PJ, Hu Y, Taliana L, Krauss RS: BOC, an Ig superfamily member, associates with CDO to positively regulate myogenic differentiation. EMBO J 2002;21:114–124.
12 Gibson UE, Heid CA, Williams PM: A novel method for real time quantitative RT-PCR. Genome Res 1996;6:995–1001.
13 Kondo T, Oue N, Yoshida K, et al: Expression of POT1 is associated with tumor stage and telomere length in gastric carcinoma. Cancer Res 2004;64:523–529.
14 Yasui W, Sano T, Nishimura K, et al: Expression of P-cadherin in gastric carcinomas and its reduction in tumor progression. Int J Cancer 1993;54:49–52.
15 Alley MC, Scudiero DA, Monks A, et al: Feasibility of drug screening with panels of human tumor cell lines using a microculture tetrazolium assay. Cancer Res 1988;48:589–601.
16 Sakamoto N, Oue N, Noguchi T, et al: Serial analysis of gene expression of esophageal squamous cell carcinoma: ADAMTS16 is upregulated in esophageal squamous cell carcinoma. Cancer Sci 2010;101:1038–1044.
17 Challita-Eid PM, Morrison K, Etessami S, et al: Monoclonal antibodies to six-transmembrane epithelial antigen of the prostate-1 inhibit intercellular communication in vitro and growth of human tumor xenografts in vivo. Cancer Res 2007;67:5798–5805.
18 Fritzsche FR, Jung M, Tölle A, et al: ADAM9 expression is a significant and independent prognostic marker of PSA relapse in prostate cancer. Eur Urol 2008;54:1097–1106.
19 Izumi Y, Hirata M, Hasuwa H, et al: A metalloprotease-disintegrin, MDC9/meltrin-γ/ADAM9 and PKCδ are involved in TPA-induced ectodomain shedding of membrane-anchored heparin-binding EGF-like growth factor. EMBO J 1998;17:7260–7272.
20 Peduto L, Reuter VE, Shaffer DR, Scher HI, Blobel CP: Critical function for ADAM9 in mouse prostate cancer. Cancer Res 2005;65:9312–9319.
21 Josson S, Anderson CS, Sung SY, et al: Inhibition of ADAM9 expression induces epithelial phenotypic alterations and sensitizes human prostate cancer cells to radiation and chemotherapy. Prostate 2011;71:232–240.
22 McLellan JS, Zheng X, Hauk G, Ghirlando R, Beachy PA, Leahy DJ: The mode of Hedgehog binding to Ihog homologues is not conserved across different phyla. Nature 2008;455:979–983.
23 Zhang W, Kang JS, Cole F, Yi MJ, Krauss RS: CDO functions at multiple points in the Sonic Hedgehog pathway, and CDO-deficient mice accurately model human holoprosencephaly. Dev Cell 2006;10:657–665.
24 Pasca di Magliano M, Hebrok M: Hedgehog signalling in cancer formation and maintenance. Nat Rev Cancer 2003;3:903–911.
25 Bale AE: Hedgehog signaling and human disease. Annu Rev Genomics Hum Genet 2002;3:47–65.
26 Sanchez P, Hernández AM, Stecca B, et al: Inhibition of prostate cancer proliferation by interference with SONIC HEDGEHOG-GLI1 signaling. Proc Natl Acad Sci USA 2004;101:12561–12566.

Editorial

Pathobiology

Pathobiology 2011;78:293–294
DOI: 10.1159/000331226

Future Perspectives of Gastric Cancer Treatment – From Bench to Bedside

Cancer, a chronic proliferative disease with multiple genetic and epigenetic alterations, develops as a result of an accumulation of various endogenous and exogenous causes. Recent advances in cancer research have uncovered the molecular mechanisms of the development and progression of the disease. Multiple alterations during carcinogenesis are found in tumor suppressor genes, oncogenes, DNA repair genes, cell cycle regulators, cell adhesion molecules, growth factors/receptors, matrix metalloproteinases and other sites. Because of different but also common molecular bases, each cancer displays a different biological behavior and response to treatment. Recent focus has been on the presence of cancer stem cells in terms of chemoradiotherapy.

Amongst 10 million people diagnosed with cancer in the world, the most common cancers are those of the lung, breast and stomach. However, there are marked regional differences in the organs that are affected. In eastern Asia including Japan, Korea and China, cancers of the stomach, lung, liver and esophagus are of major concern, although cancers of the breast and colorectum are also increasing. Mortality due to gastric cancer, one of the most common cancers worldwide, is second to lung cancer. The highest rates of gastric cancer occur in eastern Asia, South America and Eastern Europe. Of particular note, more than half of the gastric cancer in the world occurs in Japan, China and Korea. Advances in diagnosis and treatment have enabled us to offer excellent long-term survival for early cancer, but the prognosis for advanced cancer still remains poor. The International Gastric Cancer Association, founded in 1995, contributes greatly to research into the carcinogenesis, diagnosis and treatment of gastric cancer; a congress on these issues was held recently, in 2011, in Seoul, Korea. Many scientific events on gastric cancer have been organized in these countries, such as the international symposium 'Future Perspectives of Gastrointestinal Cancer Treatment – From Bench to Bedside' at the occasion of the 20th Annual Meeting of the Japanese Society for Gastroenterological Carcinogenesis, the 17th Seoul International Cancer Symposium 'Gastric Cancer Update 2010', among others.

In this issue of *Pathobiology*, distinguished experts in Asia review current topics and future perspectives of gastric cancer treatment in molecular pathology, tissue engineering, surgery and chemotherapy. Woo et al. present the biological significance of STAT3 activation in gastric cancer. They analyzed a large number of gastric cancer specimens on tissue arrays immunohistochemically using several antibodies including anti-phospho-Tyr705-STAT3, an active form of STAT3. Nuclear STAT3 activation was an early event in carcinogenesis and significantly correlated with better prognosis, proliferation and HIF-1α activation in gastric cancer, suggesting that the nuclear pSTAT3 may serve as a valuable prognostic factor and therapeutic target in gastric carcinoma. Jang and Kim review the recent understanding of the molecular pathology of gastric cancer. Gastric cancer develops through multistep processes that begin with *Helicobacter pylori*-induced atrophic gastritis. Genetic and epigenetic

KARGER

Fax +41 61 306 12 34
E-Mail karger@karger.ch
www.karger.com

1015–2008/11/0786–0293$38.00/0

Accessible online at:
www.karger.com/pat

alterations include TP53, CTNNB1 and Runx3. Gastric cancer with microsatellite instability is a well-defined subset exhibiting distinctive clinicopathological features. Targeted therapy using trastuzumab against gastric cancer with ERBB2/*HER2* amplification shows a better prognosis. A genome-wide search to identify novel methylation-silenced genes will provide novel opportunities in the treatment of gastric cancer. For the treatment of early cancer of the upper gastrointestinal tract, endoscopic submucosal dissection is widely used. Takagi et al. describe the usefulness of autologous oral mucosal epithelial cell sheets to prevent stenosis after esophageal endoscopic submucosal dissection. Human oral mucosal epithelial cells can be successfully cultured and harvested as continuous cell sheets without any animal-derived materials. The method for fabricating epithelial cell sheets shown here is suitable for the validation for clinical trials. Yang describes the importance of translational research in the clinical field and of answering the questions of the operating room by basic research. The clinical questions include the source of disseminated cancer cells during gastric surgery, the implications of serum gastrin level after proximal gastrectomy and the exploration of local drug delivery systems for gastric cancer. Various concepts and technologies, such as epigenetics, microRNA, genetic polymorphism and the microarray technique, have contributed to uncovering molecular stomach carcinogenesis. The next generation of sequencing is a promising revolutionary tool. Isogaki et al. discuss the outline of robot-assisted surgery for gastric cancer. The da Vinci surgical system was developed for minimally invasive surgery. While the procedures of the gastrectomy are similar to those of the usual laparoscopic surgery, several aspects such as the port placement and the role of the assistant are modified. Robot-assisted gastrectomy using the da Vinci system can be applied safely and effectively for the treatment of advanced gastric cancer even with lymph node dissection. Higuchi et al. review the current status of chemotherapy for gastric cancer and discuss future perspectives. Numerous randomized trials of various chemotherapeutic regimens have contributed to improved outcomes in patients with advanced gastric cancer. The standard regimen for advanced gastric cancer in Japan is a combination of S-1 and cisplatin. Recently, new drug development has focused on molecular target agents, and personalized therapy for advanced gastric cancer has just begun. Since abundant information about the heterogeneity and biological background of gastric cancer has been compiled, new strategies for personalized therapy will be introduced in the future. Yoshida et al. describe the roles of surgical oncologists in the new era. Surgical oncologists have two main roles in the treatment of gastric cancer. One is to provide minimally invasive surgery for early gastric cancer patients and the new concept of surgical intervention for advanced and metastatic disease. The second is to evaluate the significant values of the aggressive treatment, called 'adjuvant surgery', for stage IV gastric cancer patients who have successfully responded to initial chemotherapy for curative intent.

In conclusion, this issue of *Pathobiology* presents reviews of the current status and the future perspectives of the pathology, research and treatment of gastric cancer. A detailed understanding of the molecular pathogenesis and individual character of gastric cancer will contribute to providing personalized cancer care. The new development of medical technologies and therapeutic agents will enable us to provide the best treatment for patients of both early and advanced cancer. The viewpoints from bench to bedside and clinic to bench are absolutely crucial.

Wataru Yasui

Serum concentration and expression of Reg IV in patients with esophageal cancer: Age-related elevation of serum Reg IV concentration

NAOHIDE OUE[1], TSUYOSHI NOGUCHI[2], KATSUHIRO ANAMI[1], KAZUHIRO SENTANI[1], NAOYA SAKAMOTO[1], NAOHIRO URAOKA[1], YUTA WAKAMATSU[1], HIROKI SASAKI[3] and WATARU YASUI[1]

[1]Department of Molecular Pathology, Hiroshima University Graduate School of Biomedical Sciences, Hiroshima;
[2]Department of Gastrointestinal Surgery, Oita University Faculty of Medicine, Oita;
[3]Genetics Division, National Cancer Center Research Institute, Tokyo, Japan

Received September 29, 2010; Accepted December 29, 2010

DOI: 10.3892/ol.2011.239

Abstract. *Regenerating islet-derived family, member 4* (*REG4*, which encodes Reg IV) is a marker for cancer and inflammatory bowel disease. This study aimed to investigate the diagnostic utility of Reg IV measurement in sera from esophageal cancer patients. Reg IV expression was examined in 269 esophageal cancer samples by immunostaining and the Reg IV levels in sera were measured from 65 patients with esophageal squamous cell carcinoma (SCC) by enzyme-linked immunosorbent assay. No Reg IV staining was detected in 255 SCC and 4 small cell carcinoma samples, whereas Reg IV was stained in 4 of 10 (40%) adenocarcinoma samples. Serum Reg IV concentration in esophageal SCC patients was significantly higher compared to that of the control subjects (P=0.0003). A significant correlation between serum Reg IV concentration and age was found in control subjects (P<0.0001). When serum Reg IV concentration was analyzed according to age, the distribution of serum Reg IV concentration in patients with esophageal SCC was similar to that of the control subjects. These results suggest that Reg IV expression is highly specific for adenocarcinoma of the esophagus. Further investigation is required to clarify whether Reg IV serves as a serum tumor marker for esophageal cancer.

Introduction

Regenerating islet-derived family, member 4 (*REG4*, which encodes Reg IV) is a member of the *REG* gene family, which constitutes a multi-gene family belonging to the calcium-dependent lectin superfamily. *REG4* was originally identified by high-throughput sequence analysis of a large inflammatory bowel disease cDNA library (1). Previously a serial analysis of gene expression in four primary gastric cancer tissues was performed and a number of gastric cancer-specific genes were identified (2,3). Of these genes, *REG4* is a candidate gene for cancer-specific expression in patients with gastric cancer. Our previous immunohistochemical analysis showed that Reg IV was expressed in 30% of gastric cancers and was associated with intestinal mucin phenotype and neuroendocrine differentiation (4). A number of immunohistochemical analyses of Reg IV have been reported in human cancers, including lung, breast, pancreas, colorectal, prostate, salivary gland, kidney, urinary bladder and gallbladder cancer (4-11). These analyses indicate that Reg IV is expressed in adenocarcinoma cells showing intestinal mucin differentiation. Reg IV staining also aids in the diagnosis of gastrointestinal signet ring cell carcinoma, a unique subtype of adenocarcinoma (12). By contrast, little is known about Reg IV expression in other histological types of cancer, such as squamous cell carcinoma (SCC).

In addition to adenocarcinoma, Reg IV expression has been reported in neuroendocrine neoplasms, including gastrointestinal and renal carcinoids (4,10,13). Reg IV expression is also found in small cell carcinoma of the lung (14). However, Reg IV expression in small cell carcinoma of the esophagus has yet to be investigated.

Reg IV is a secreted protein and a novel biomarker for gastric cancer (15). The diagnostic sensitivity of serum Reg IV was superior to that of serum carcinoembryonic antigen or carbohydrate antigen 19-9. Serum Reg IV serves as a tumor marker for colorectal, pancreatic and prostate cancer (5,7,10). The data support the hypothesis that Reg IV protein is a potentially novel serum tumor marker for a wide range of malignancies. However, the serum concentration of Reg IV in esophageal cancer has yet to be measured.

In the present study, the expression and distribution of Reg IV in human esophageal cancers, including SCC, adenocarcinoma and small cell carcinoma, was examined by immunohistochemistry. Previously two Reg IV staining patterns, i.e., mucin-like and strong perinuclear staining were reported (4). Mucin-like staining is observed in goblet cells

Correspondence to: Dr Wataru Yasui, Department of Molecular Pathology, Hiroshima University Graduate School of Biomedical Sciences, 1-2-3 Kasumi, Minami-ku, Hiroshima 734-8551, Japan
E-mail: wyasui@hiroshima-u.ac.jp

Key words: Reg IV, esophageal cancer, tumor marker, immunohistochemistry

and goblet cell-like vesicles of cancer cells. These cells are positive for MUC2 (a marker of goblet cells). By contrast, strong perinuclear staining is detected in neuroendocrine cells. These cells are positive for chromogranin A (a marker of neuroendocrine cells). Therefore, the coexpression of Reg IV and MUC2 or chromogranin A was examined. Additionally, the Reg IV levels in sera from patients with esophageal cancer were measured using an enzyme-linked immunosorbent assay (ELISA) to investigate the potential diagnostic utility of Reg IV measurement.

Materials and methods

Tissue samples. Primary tumor samples from 279 patients with esophageal cancer (35 females and 244 males; age range 36-84 years, mean 65) and serum samples from 65 patients with esophageal cancer (8 females and 57 males; age range 49-82 years, mean 65) were collected. The patients had undergone curative resection between 1990 and 2002 at Oita University Hospital, Oita, Japan. Only patients without pre-operative radio- or chemotherapy and without clinical evidence of distant metastasis were enrolled in the study. The histologic classification was based on the World Health Organization system. Tumor staging was performed according to the TNM stage grouping system. For strict privacy protection, identifying information for the samples was removed prior to being analyzed in accordance with the Ethical Guidelines for Human Genome/Gene Research enacted by the Japanese Government.

For quantitative reverse transcription-polymerase chain reaction (RT-PCR), 10 primary esophageal cancer tissue samples and their corresponding non-neoplastic mucosa samples were used. The 10 esophageal cancer samples were all SCC. The samples were obtained at the time of resection, immediately frozen in liquid nitrogen and stored at -80˚C until use. It was microscopically confirmed that the tumor specimens consisted mainly (>50%) of carcinoma tissue.

The 269 primary esophageal cancer tissue samples were used for immunohistochemical analysis. The samples were archival formalin-fixed, paraffin-embedded tissues. These 269 esophageal cancer samples were classified histologically as SCC (n=255), adenocarcinoma (n=10) or small cell carcinoma (n=4).

Serum samples were used to measure Reg IV levels using ELISA. All 65 serum samples were obtained from patients with esophageal SCC prior to surgery and before initiation of therapy. Primary esophageal SCC tissue samples from all 65 patients with esophageal cancer were available for immunohistochemical analysis. The control serum samples were obtained from 133 healthy individuals (92 females and 41 males; age range 21-80 years, mean 51). Control subjects were randomly selected from individuals visiting hospitals for regular health checks or due to certain symptoms, such as appetite loss or epigastralgia. The control subjects were confirmed to be free of malignancy by gastrointestinal endoscopy and biopsy. The serum samples were stored at -80˚C until analysis.

Quantitative RT-PCR. Total RNA was extracted with an RNeasy mini kit (Qiagen, Valencia, CA, USA) and 1 μg of total RNA was converted to cDNA with a First Strand cDNA synthesis kit (Amersham Biosciences, Piscataway, NJ, USA). Quantitation of *REG4* mRNA levels was performed by real-time fluorescence detection as previously described (2). In brief, PCR was performed with a SYBR-Green PCR Core Reagents kit (Applied Biosystems, Foster City, CA, USA). Real-time detection of the emission intensity of SYBR-Green bound to double-stranded DNA was performed with an ABI PRISM 7700 Sequence Detection System (Applied Biosystems) as previously described (16). ACTB-specific PCR products were amplified from the same RNA samples and served as an internal control.

Immunohistochemistry. Formalin-fixed, paraffin-embedded samples were sectioned, deparaffinized and stained with hematoxylin and eosin to ensure that the sectioned block contained tumor cells. Adjacent sections were then stained immunohistochemically. The sections were pre-treated by microwaving in citrate buffer for 30 min to retrieve antigenicity. After peroxidase activity was blocked with 3% H_2O_2-methanol for 10 min, the sections were incubated with normal goat serum (Dako, Carpinteria, CA, USA) for 20 min to block non-specific antibody binding. The sections were incubated with a primary antibody against Reg IV (rabbit polyclonal antibody, diluted 1:50; anti-Reg IV antibody was raised and characterized in our laboratory) (4), MUC2 (1:50; Novocastra, Newcastle, UK) or chromogranin A (1:50; Novocastra) for 1 h at room temperature, followed by incubation with peroxidase-labeled anti-rabbit or anti-mouse IgG for 1 h. Staining was completed with a 10-min incubation in a substrate-chromogen solution. The sections were counterstained with 0.1% hematoxylin. The specificity of the Reg IV antibody was previously characterized (4). Staining of each antibody was considered positive if any tumor cells were stained.

Enzyme-linked immunosorbent assay. For the measurement of serum Reg IV concentration, a sandwich ELISA method was developed as previously described (15). First, polystyrene microtiter plates were coated with mouse monoclonal anti-Reg IV antibody (R&D Systems, Abingdon, UK) by overnight incubation of 50 μl/125 ng/well antibody diluted in Tris buffer (pH 7.4). The plates were then washed three times with wash buffer. After the plates were blocked with 1% milk in phosphate-buffered saline, 50 μl of recombinant Reg IV standard or sample was added to each well and incubated overnight at 4˚C. After three washes, 50 μl of biotinylated goat polyclonal anti-Reg IV antibody (R&D Systems) in assay buffer [1% bovine serum albumin (BSA), Tris buffer (pH 7.4) and 0.05% normal goat serum] was added to each well (75 ng antibody/well). The mixture was then incubated for 1 h with agitation at 37˚C and washed three times with wash buffer. The plates were incubated with 50 μl/well alkaline phosphatase-conjugated streptavidin (Dako) diluted 1:2,000 in diluent containing 1% BSA and Tris buffer (pH 7.4) for 1 h at 37˚C and washed three times. Color development was performed with the addition of pNPP chromogenic substrate (Sigma-Aldrich, St. Louis, MO, USA) followed by incubation at 37˚C for 1 h. Absorbance at 405 nm was measured with an ELISA plate reader. As a reference standard, known concentrations of human recombinant Reg IV from 0 to 30 ng/ml were tested in triplicate.

Statistical methods. Differences in the serum Reg IV concentration between two groups were tested using the non-

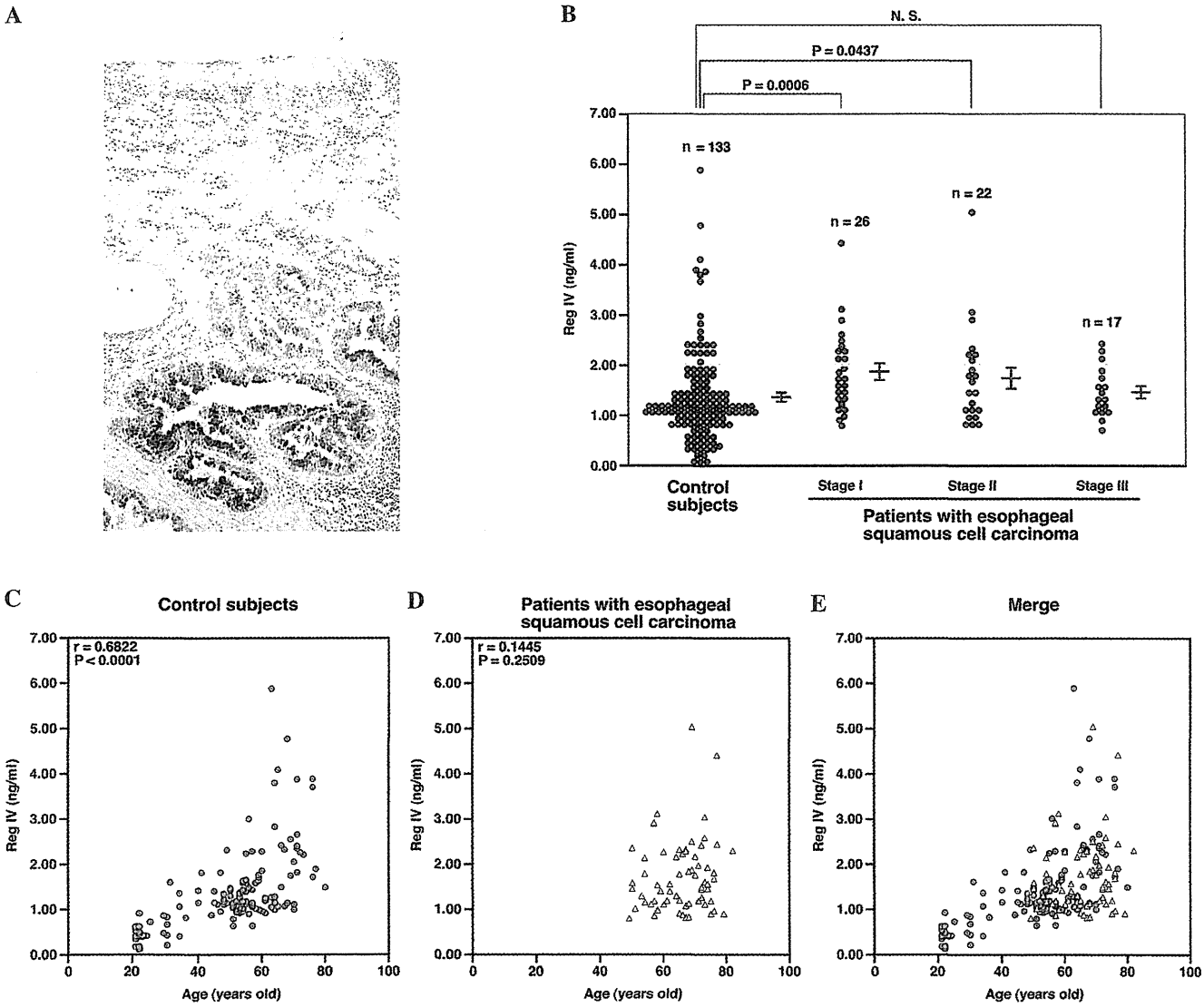

Figure 1. Immunostaining and serum concentration of Reg IV in esophageal cancer. (A) Immunostaining of Reg IV in esophageal adenocarcinoma (original magnification, x100). Reg IV staining is observed in goblet cell-like vesicles of adenocarcinoma cells. (B) Enzyme-linked immunosorbent assay of serum samples from 133 control subjects and 65 patients with esophageal squamous cell carcinoma (SCC). The yellow bar indicates the cut-off levels defined on the basis of a previous study (2 ng/ml) (15). The red bars indicate the mean ± SE. Differences in the serum concentration of Reg IV between two groups were tested using the Mann-Whitney U test. (C) Correlation between the serum concentrations of Reg IV and age in control subjects. The correlation was examined using Spearman's rank correlation test. (D) Correlation between the serum concentrations of Reg IV and age in patients with esophageal SCC. The correlation was examined using Spearman's rank correlation. (E) Panel (C) was merged with panel (D).

parametric Mann-Whitney U test. Correlations between the serum Reg IV concentration and age or gender were assessed using Spearman's rank correlation test. $P<0.05$ was considered to be statistically significant.

Results

Expression of Reg IV in esophageal cancer. An immunohistochemical analysis of Reg IV was performed in 269 human esophageal cancer tissue samples. Although esophageal SCC is the most frequent subtype of esophageal cancer in Asian countries, no Reg IV staining was detected in any of the 255 esophageal SCC samples. Quantitative RT-PCR of *REG4* was performed in 10 esophageal SCC samples; however, no *REG4* expression was found. By contrast, Reg IV was stained in 4 of 10 (40%) adenocarcinoma samples (Fig. 1A). The Reg IV staining was mucin-like; no perinuclear staining was noted. It was confirmed that tumor cells showing mucin-like staining of Reg IV were positive for MUC2 and negative for chromogranin A (data not shown). Although extensive chromogranin A staining was observed in the 4 samples of small cell carcinoma, no Reg IV staining was found (data not shown). Reg IV staining was also not found in corresponding non-neoplastic squamous cells (Fig. 1A).

Serum Reg IV concentration in patients with esophageal squamous cell carcinoma and control subjects. Serum Reg IV levels in 133 control subjects and 65 patients with esophageal SCC measured by ELISA are shown in Fig. 1B. The serum Reg IV concentration of control subjects measured in the

present study (mean ± SE, 1.38±0.08 ng/ml) was higher than that measured in our previous study (0.52±0.05 ng/ml) (15). The correlation between the serum concentration of Reg IV and age or gender was investigated. Although the serum concentration of Reg IV did not correlate with age in our previous study (15), serum concentration was higher in elderly compared to that in young control subjects. Spearman's rank correlation test showed a significant correlation between serum Reg IV and age (r=0.4362, P<0.0001) (Fig. 1C). In our previous study, the cut-off level for Reg IV was set at 2 ng/ml (15). A high level of Reg IV concentration was found in 13 of 23 (57%) control subjects who were more than 65 years old.

Serum Reg IV concentration in esophageal SCC patients at stage I (n=26, 1.88±0.16 ng/ml, P=0.0006, Mann-Whitney U test) and stage II (n=22, 1.76±0.21 ng/ml, P=0.0437, Mann-Whitney U test) was significantly higher than that of the control subjects (Fig. 1B). By contrast, the serum Reg IV concentration in esophageal SCC patients at stage III was not significantly elevated (n=17, 1.48±0.11 ng/ml, P=0.1329, Mann-Whitney U test). In total, serum Reg IV concentration in esophageal SCC patients (n=65, 1.74±0.10 ng/ml) was significantly higher compared to that of the control subjects (P=0.0003, Mann-Whitney U test).

In the present study, no Reg IV expression was detected in esophageal SCC by quantitative RT-PCR and immunohistochemistry. However, serum Reg IV concentration in esophageal SCC patients was significantly higher compared to that of the control subjects. Discrepancy between immunostaining and ELISA results is not likely due only to methodological differences. Spearman's rank correlation test showed that there was no significant correlation between serum Reg IV concentration in esophageal SCC patients and age (r=0.1445, P=0.2509) (Fig. 1D). Additionally, when the distribution of serum Reg IV concentration in esophageal SCC patients was compared to that of the control subjects, it was not significantly different (Fig. 1E).

Discussion

This study aimed to investigate the expression of Reg IV in esophageal cancer. Although Reg IV staining was not detected in esophageal SCC and small cell carcinoma samples, it was present in 40% of adenocarcinoma samples. We confirmed that the adenocarcinoma cells were also positive for MUC2. In our previous study, Reg IV expression was not found in renal cell carcinoma and was noted in only 1% of urothelial carcinoma, neither of which are adenocarcinomas (10). Taken together, these results indicate that the expression of Reg IV is highly specific for adenocarcinoma.

Although Reg IV expression was not found in esophageal SCC at the mRNA and protein levels, serum Reg IV concentrations in esophageal SCC patients at stages I and II were significantly higher compared to those of the control subjects. Spearman's rank correlation test showed a significant correlation between serum Reg IV and age in control subjects. In the ELISA analysis, the mean age of the control subjects (51 years) was younger than that of patients with esophageal SCC (65 years), suggesting that the elevation of the serum concentration of Reg IV in esophageal SCC is age-related and not due to esophageal SCC. Notably, the distribution of serum Reg IV concentration in esophageal SCC patients did not show a significant difference from that noted in the control subjects.

We are unable to thoroughly explain this age-related elevation of serum Reg IV concentration. A number of lines of evidence have suggested that Reg IV protein detected in serum samples is derived from cancer cells. In pancreatic adenocarcinoma patients, postoperative serum Reg IV levels were reduced to within normal range 3 or 4 weeks following tumor resection (5). The Reg IV concentration in serum samples from patients with gastric cancer showing Reg IV-positive immunostaining was significantly higher compared to that with gastric cancer showing Reg IV-negative immunostaining (15). Although the control subjects were confirmed to be free of malignancy by gastrointestinal endoscopy and biopsy, the possibility that the control subjects had cancer cannot be excluded. To address these issues, serum samples from cancer-free subjects confirmed by autopsy should be analyzed.

Another possible explanation for the age-related elevation of serum Reg IV concentration is Reg IV expression in intestinal metaplasia of the stomach. In our previous study, normal stomach cells were not stained by Reg IV, however, extensive staining of Reg IV was observed in intestinal metaplasia of the stomach (4). Since the incidence and prevalence of intestinal metaplasia of the stomach increase with age, age-related elevation of serum Reg IV concentration may be due to Reg IV expression in intestinal metaplasia of the stomach.

In conclusion, we showed that the expression of Reg IV is highly specific for adenocarcinoma, but is not specific for SCC or small cell carcinoma. Although serum Reg IV concentration in esophageal SCC patients was significantly higher than that in control subjects, we hypothesize that serum Reg IV is not suitable as a tumor marker for esophageal SCC detection. The reason for the apparent age-related elevation of serum Reg IV concentration in esophageal SCC patients has yet to be elucidated and further investigation is required to clarify the potential utility of serum Reg IV measurement.

Acknowledgements

We thank Mr. Shinichi Norimura for the excellent technical assistance and advice. This study was carried out with the kind cooperation of the Research Center for Molecular Medicine, Faculty of Medicine, Hiroshima University. We thank the Analysis Center of Life Science, Hiroshima University, for the use of their facilities. This study was supported in part by Grants-in-Aid for Cancer Research from the Ministry of Education, Culture, Science, Sports and Technology of Japan, and from the Ministry of Health, Labor and Welfare of Japan.

References

1. Hartupee JC, Zhang H, Bonaldo MF, Soares MB and Dieckgraefe BK: Isolation and characterization of a cDNA encoding a novel member of the human regenerating protein family: Reg IV. Biochim Biophys Acta 1518: 287-293, 2001.
2. Oue N, Hamai Y, Mitani Y, Matsumura S, Oshimo Y, Aung PP, Kuraoka K, Nakayama H and Yasui W: Gene expression profile of gastric carcinoma: identification of genes and tags potentially involved in invasion, metastasis, and carcinogenesis by serial analysis of gene expression. Cancer Res 64: 2397-2405, 2004.

3. Aung PP, Oue N, Mitani Y, Nakayama H, Yoshida K, Noguchi T, Bosserhoff AK and Yasui W: Systematic search for gastric cancer-specific genes based on SAGE data: melanoma inhibitory activity and matrix metalloproteinase-10 are novel prognostic factors in patients with gastric cancer. Oncogene 25: 2546-2557, 2006.
4. Oue N, Mitani Y, Aung PP, Sakakura C, Takeshima Y, Kaneko M, Noguchi T, Nakayama H and Yasui W: Expression and localization of Reg IV in human neoplastic and non-neoplastic tissues: Reg IV expression is associated with intestinal and neuroendocrine differentiation in gastric adenocarcinoma. J Pathol 207: 185-198, 2005.
5. Takehara A, Eguchi H, Ohigashi H, Ishikawa O, Kasugai T, Hosokawa M, Katagiri T, Nakamura Y and Nakagawa H: Novel tumor marker REG4 detected in serum of patients with resectable pancreatic cancer and feasibility for antibody therapy targeting REG4. Cancer Sci 97: 1191-1197, 2006.
6. Nakata K, Nagai E, Ohuchida K, Aishima S, Hayashi A, Miyasaka Y, Yu J, Mizumoto K, Tanaka M and Tsuneyoshi M: REG4 is associated with carcinogenesis in the 'intestinal' pathway of intraductal papillary mucinous neoplasms. Mod Pathol 22: 460-468, 2009.
7. Oue N, Kuniyasu H, Noguchi T, Sentani K, Ito M, Tanaka S, Setoyama T, Sakakura C, Natsugoe S and Yasui W: Serum concentration of Reg IV in patients with colorectal cancer: overexpression and high serum levels of Reg IV are associated with liver metastasis. Oncology 72: 371-380, 2007.
8. Ohara S, Oue N, Matsubara A, Mita K, Hasegawa Y, Hayashi T, Usui T, Amatya VJ, Takeshima Y, Kuniyasu H and Yasui W: Reg IV is an independent prognostic factor for relapse in patients with clinically localized prostate cancer. Cancer Sci 99: 1570-1577, 2008.
9. Sasahira T, Oue N, Kirita T, Luo Y, Bhawal UK, Fujii K, Yasui W and Kuniyasu H: Reg IV expression is associated with cell growth and prognosis of adenoid cystic carcinoma in the salivary gland. Histopathology 53: 667-675, 2008.
10. Hayashi T, Matsubara A, Ohara S, Mita K, Hasegawa Y, Usui T, Arihiro K, Norimura S, Sentani K, Oue N and Yasui W: Immunohistochemical analysis of Reg IV in urogenital organs: Frequent expression of Reg IV in prostate cancer and potential utility as serum tumor marker. Oncol Rep 21: 95-100, 2009.
11. Tamura H, Ohtsuka M, Washiro M, Kimura F, Shimizu H, Yoshidome H, Kato A, Seki N and Miyazaki M: Reg IV expression and clinicopathologic features of gallbladder carcinoma. Hum Pathol 40: 1686-1692, 2009.
12. Sentani K, Oue N, Tashiro T, Sakamoto N, Nishisaka T, Fukuhara T, Taniyama K, Matsuura H, Arihiro K, Ochiai A and Yasui W: Immunohistochemical staining of Reg IV and claudin-18 is useful in the diagnosis of gastrointestinal signet ring cell carcinoma. Am J Surg Pathol 32: 1182-1189, 2008.
13. Sentani K, Oue N, Noguchi T, Sakamoto N, Matsusaki K and Yasui W: Immunostaining of gastric cancer with neuroendocrine differentiation: Reg IV-positive neuroendocrine cells are associated with gastrin, serotonin, pancreatic polypeptide and somatostatin. Pathol Int 60: 291-297, 2010.
14. Heiskala K, Arola J, Heiskala M and Andersson LC: Expression of Reg IV and Hath1 in neuroendocrine neoplasms. Histol Histopathol 25: 63-72, 2010.
15. Mitani Y, Oue N, Matsumura S, Yoshida K, Noguchi T, Ito M, Tanaka S, Kuniyasu H, Kamata N and Yasui W: Reg IV is a serum biomarker for gastric cancer patients and predicts response to 5-fluorouracil-based chemotherapy. Oncogene 26: 4383-4393, 2007.
16. Kondo T, Oue N, Yoshida K, Mitani Y, Naka K, Nakayama H and Yasui W: Expression of POT1 is associated with tumor stage and telomere length in gastric carcinoma. Cancer Res 64: 523-529, 2004.

UICC
global cancer control

IJC
International Journal of Cancer

Anti-stromal therapy with imatinib inhibits growth and metastasis of gastric carcinoma in an orthotopic nude mouse model

Tomonori Sumida[1], Yasuhiko Kitadai[1], Kei Shinagawa[1], Miwako Tanaka[1], Michiyo Kodama[1], Mayu Ohnishi[1], Eiji Ohara[1], Shinji Tanaka[2], Wataru Yasui[3] and Kazuaki Chayama[1]

[1] Department of Medicine and Molecular Science, Graduate School of Biomedical Sciences, Hiroshima University, Hiroshima, Japan
[2] Department of Endoscopy, Hiroshima University Hospital, Hiroshima, Japan
[3] Department of Molecular Pathology, Graduate School of Biomedical Sciences, Hiroshima University, Hiroshima, Japan

Recent studies have revealed that platelet-derived growth factor (PDGF) plays a role in promoting progressive tumor growth in several organs; however, whether PDGF plays such a role in gastric carcinoma is undetermined. We examined whether inhibition of PDGF receptor (PDGF-R) tyrosine kinase signaling by imatinib affects tumor growth and metastasis in an orthotopic nude mouse model of human gastric carcinoma. TMK-1 human gastric carcinoma cells were injected into the gastric wall of nude mice. Groups of mice (n = 10 each) received sterile water (control), low-dose imatinib (50 mg/kg/day), high-dose imatinib (200 mg/kg/day), cancer chemotherapeutic agent irinotecan (5 mg/kg/week), or imatinib (50 mg/kg/day or 200 mg/kg/day) and irinotecan (5 mg/kg/week) in combination for 28 days. Tumor growth and metastasis were assessed. Resected tumors were analyzed immunohistochemically. Carcinoma-associated fibroblasts, pericytes and lymphatic endothelial cells in stroma expressed high levels of PDGF-R; carcinoma cells did not. Treatment with imatinib alone did not inhibit tumor growth and metastasis; however, treatment with irinotecan alone or combined with imatinib significantly inhibited tumor growth. Only treatment with high-dose imatinib and irinotecan in combination inhibited lymph node and peritoneal metastases. Immunohistochemically, only imatinib alone or in combination with irinotecan was shown to significantly decrease the stromal reaction, microvessel area and pericyte coverage of tumor microvessels. These effects were marked with high-dose imatinib. In conclusion, administration of PDGF-R tyrosine kinase inhibitor in combination with irinotecan appears to impair the progressive growth of gastric carcinoma by blockade of PDGF-R signaling pathways in stromal cells.

Recent studies in tumor biology have shown that tumor growth and metastasis are determined not only by cancer cells, but also by a variety of stromal cells. The stroma constitutes a large part of most solid tumors, and the cancer-stromal cell interaction contributes functionally to tumor growth and metastasis.[1,2] Tumor stroma contains many different cell types, including activated fibroblasts (myofibroblasts), endothelial cells and inflammatory cells. It has become clear that activated fibroblasts in cancer stroma are prominent modifiers of tumor progression. As such, they are called carcinoma-associated fibroblasts (CAFs).[3] Although the mechanisms that regulate activation of fibroblasts and their accumulation in tumors are not fully understood, platelet-derived growth factor (PDGF), transforming growth factor-β and fibroblast growth factor (FGF)-2 are known to be partly involved in this process.[4]

PDGF and PDGF receptor (PDGF-R) are expressed in many types of human neoplasm, including neoplasm of the prostate,[5] lung,[6] colon[7] and breast.[8,9] PDGF is a dimeric protein of the following molecular variants: PDGF-AA, PDGF-BB, PDGF-AB, PDGF-CC and PDGF-DD.[10] The α-receptor binds all possible forms of PDGF except PDGF-DD, whereas PDGF-Rβ preferentially binds PDGF-BB. PDGF-R signaling is reported to increase proliferation of tumor cells in an autocrine manner[11] and to stimulate angiogenesis,[12] recruit pericytes[11,13] and control interstitial fluid pressure (IFP) in stroma, influencing transvascular transport of chemotherapeutic agents in a paracrine manner.[14] Receptor tyrosine kinases have been proposed as potential targets for antitumor therapy. Imatinib mesylate (also known as STI571 or Gleevec) is a protein-tyrosine kinase inhibitor of the 2-phenylaminopyrimidine class that was developed initially for its

Key words: gastric carcinoma, platelet-derived growth factor receptor, carcinoma-associated fibroblast
Grant sponsors: Ministry of Education, Culture, Science, Sports and Technology of Japan (Grants-in-Aid for Cancer Research), Ministry of Health, Labor and Welfare of Japan
DOI: 10.1002/ijc.25812
History: Received 7 May 2010; Accepted 11 Nov 2010; Online 2 Dec 2010
Correspondence to: Yasuhiko Kitadai, Department of Medicine and Molecular Science, Graduate School of Biomedical Sciences, Hiroshima University, 1-2-3 Kasumi, Minami-ku, Hiroshima 734-8551, Japan, Tel: +81-82-257-5193, Fax: +81-82-257-5194, E-mail: kitadai@hiroshima-u.ac.jp

selectivity against Bcr-Abl fusion protein present in nearly all patients with chronic myeloid leukemia.[15] Additional tyrosine kinases are inhibited by imatinib: c-kit, the receptor for kit ligand (KL) and two structurally similar PDGF-Rs (PDGF-Rα and PDGF-Rβ) and DDRs (DDR1 and DDR2).[16,17] Imatinib therapy is well tolerated and leads to remission in patients with c-kit-positive gastrointestinal stromal tumor containing gain-of-function mutations in c-kit.[18] Imatinib is also reported to inhibit the growth of glioblastoma, dermatofibrosarcoma protuberans, neuroblastoma, Ewing's sarcoma and small cell lung cancer, all of which may exhibit PDGF/PDGF-R or KL/c-kit autocrine growth loops.[19–23] It was reported recently that blockade of paracrine PDGF-R signaling pathways in tumor-associated endothelial cells could serve as a novel therapy for many neoplasms.[24,25] In addition to endothelial cells that form the tumor vasculature, attention is now focused on other elements of the stromal compartment, *i.e.*, CAFs and vascular pericytes.[26]

In this study, we examined the therapeutic effect of imatinib administered as a single agent or in combination with chemotherapeutic agent irinotecan against human gastric carcinoma cells growing in an orthotopic nude mice model, paying particular attention to tumor stroma. Irinotecan has been evaluated alone and in combined therapy in multiple trials, with promising results and good tolerance in patients with advanced gastric carcinoma.[27]

Material and Methods

Human gastric carcinoma cell lines and culture conditions

The TMK-1 cell line (poorly differentiated adenocarcinoma) was kindly provided by Dr. E. Tahara (Hiroshima University, Hiroshima, Japan). The KKLS cell line (undifferentiated carcinoma) was kindly provided by Dr. Y. Takahashi (Chiba University, Chiba, Japan). Human osteosarcoma cell line MG63 (positive control for PDGF-R expression) was obtained from the Health Science Research Resources Bank, Osaka, Japan. These cell lines were maintained in RPMI 1640 (Nissui Co., Tokyo, Japan) with 10% fetal bovine serum (FBS; Sigma, St. Louis, MO).

Semiquantitative reverse transcription polymerase chain reaction

Total RNA was extracted from gastric carcinoma cell lines with an RNeasy Kit (Qiagen, Tokyo, Japan) according to the manufacturer's instructions. Reverse transcription polymerase chain reaction (RT-PCR) was performed with the isolated RNA (1 μg). cDNA was generated from 1 μg of total RNA with a first-strand cDNA synthesis kit (Amersham Biosciences, Buckinghamshire, UK). Semi-quantitative RT-PCR was performed with an AmpliTag Gold Kit (Roche, Mannheim, Germany) according to the manufacturer's instructions. RT-PCR reactions without reverse transcription showed no specific bands. Respective primer sequences, annealing temperatures and PCR cycles were as follows: PDGF-B forward, CGAGTTGGACCTGAACATGA and PDGF-B reverse, GTCACCGTGGCCTTCTTAAA (PDGF-B PCR product, 339 bp; 58°C; 30 cycles); PDGF-Rβ forward, AGCTACCCCT CAAGGAATCATAG and PDGF-Rβ reverse, CTCTG GTGGATGGATTAAGACTG (PDGF-Rβ PCR product, 376 bp; 58°C; 30 cycles); and GAPDH forward, ATCATCC CTGCCTCTACTGG and GAPDH reverse, CCCTCCG ACGCCTGCTTCAC (GAPDH PCR product, 188 bp; 58°C; 28 cycles).

Reagents

Imatinib (imatinib mesylate or Gleevec; Novartis Pharma, Basel, Switzerland) was diluted in sterile water for oral administration. Irinotecan (Camptosar; Pharmacia, North Peapack, NJ) was kept at room temperature and dissolved in 0.9% NaCl on the day of intraperitoneal injection. Primary antibodies were purchased as follows: polyclonal rabbit anti-PDGF-Rβ, polyclonal rabbit anti-phosphorylated PDGF-Rβ (p-PDGF-Rβ), polyclonal rabbit anti-PDGF-BB subunit from Santa Cruz Biotechnology (Santa Cruz, CA); rat anti-mouse CD31 from BD PharMingen (San Diego, CA); mouse anti-desmin monoclonal antibody from Molecular Probes (Eugene, OR); α-smooth muscle actin (α-SMA) and Ki-67 equivalent antibody (MIB-1) from Dako Cytomation (Carpinteria, CA); monoclonal rat anti-mouse Lyve-1 antibody from R&D Systems (Minneapolis, MN) and polyclonal rabbit anti-mouse type-1 collagen from Novotec (Saint Martin La Garenne, France). The following fluorescent secondary antibodies were used: Alexa 488-conjugated goat anti-rabbit IgG, Alexa 488-conjugated goat anti-rat IgG and Alexa 546-conjugated goat anti-rabbit IgG (all from Molecular Probes).

Western blot analysis

Gastric carcinoma cell lines and MG63 cells were cultured in serum-free culture medium for 1 hr and then stimulated with 10 ng/mL PDGF-BB for 10 min. After three washes with cold phosphate-buffered saline (PBS) containing 1 mmol/L sodium orthovanadate, cells were lysed. Proteins (total protein 20 μg) were separated by SDS-PAGE and transferred to nitrocellulose transfer membranes (Whatman GmbH, Dassel, Germany). The immune complexes were visualized by enhanced chemiluminescence with an ECL Plus Kit (GE Healthcare, Buckinghamshire, UK).

Cell proliferation assay

In vitro growth was measured with a Cell Proliferation Biotrak ELISA System, version 2 (Amersham Biosciences, Piscataway, NJ), according to the manufacturer's instructions. Cells were seeded in a 96-well plate at a density of 1×10^4 cells/well and incubated overnight in 200 μL culture medium containing 10% FBS. After incubation for 24 hr, cells were cultured in serum-free culture medium containing 10 μM BrdU with or without imatinib for 24 hr, and cell proliferation was measured in a plate reader (Microplate Manager 5.2.1, BIO-RAD, Hercules, CA) at 450 nm.

Animals and orthotopic implantation of tumor cells

Male athymic nude BALB/c mice were obtained from Charles River Japan (Tokyo, Japan). The mice were maintained under specific pathogen-free conditions and used at 5 weeks of age. The study was carried out after permission was granted by the Committee on Animal Experimentation of Hiroshima University. KKLS and TMK-1 cells were harvested from subconfluent cultures by brief exposure to 0.25% trypsin and 0.02% ethylenediamine tetraacetic acid. Trypsinization was stopped with medium containing 10% FBS, and the cells were washed once in serum-free medium and resuspended in Hanks' balanced salt solution (HBSS). Only suspensions consisting of single cells with >90% viability were used. To produce gastric tumors, 1×10^6 cells in 50 μL of HBSS were injected into the gastric wall in nude mice under observation with a zoom stereomicroscope.

Treatment of established human gastric carcinoma tumors growing in the gastric wall in nude mice

To evaluate the therapeutic effects of imatinib on stromal cells, we performed preliminary dose-response experiments (optimal biological dose as determined previously).[28–30] Fourteen days after the orthotopic implantation of tumor cells, mice were randomized into three groups: those given water daily (control group), those given 50 mg/kg/day imatinib by oral gavage and those given 200 mg/kg/day imatinib by oral gavage. Treatments continued for 28 days, and the mice were killed on day 29. Excised tumors were used for immunohistochemical analysis.

To evaluate the effect of combination therapy, in a second experiment, mice were randomized to receive 1 of the following 6 treatments ($n = 10$ in each group): (*i*) daily administration of water by oral gavage and weekly intraperitoneal injection of PBS (control group), (*ii*) daily oral gavage of low-dose imatinib (50 mg/kg) and weekly intraperitoneal injection of PBS, (*iii*) daily oral gavage of high-dose imatinib (200 mg/kg) and weekly intraperitoneal injection of PBS, (*iv*) daily oral gavage of water and weekly intraperitoneal injection of irinotecan (5 mg/kg), (*v*) daily oral gavage of low-dose imatinib (50 mg/kg) and weekly intraperitoneal injection of irinotecan (5 mg/kg), (*vi*) daily oral gavage of high-dose imatinib (200 mg/kg) and weekly intraperitoneal injection of irinotecan (5 mg/kg). The mice were treated for 28 days, then killed and subjected to necropsy.

Necropsy procedures and histologic studies

Mice bearing orthotopic tumors were euthanized by methophane. Body weights were recorded. After necropsy, tumors were excised and weighed. For immunohistochemical and hematoxylin and eosin (H&E) staining, one part of the tumor tissue was fixed in formalin and embedded in paraffin, and the other part was embedded in OCT compound (Miles, Elkhart, IN), rapidly frozen in liquid nitrogen and stored at −80°C. All macroscopically enlarged regional (celiac and para-aortal) lymph nodes were harvested, and the presence of metastatic disease was confirmed by histologic examination.

Double immunofluorescence staining for PDGF-Rβ and α-SMA (CAFs), CD31 (vascular endothelial cells), Lyve-1 (lymphatic endothelial cells) or desmin (pericytes)

Fresh-frozen specimens of TMK-1 human gastric carcinoma tissue obtained from nude mice were cut into 8-μm sections and mounted on positively charged slides. In preparation for assays, sections were fixed in ice-cold acetone for 10 min, then washed thrice with PBS for 3 min each. Slides were placed in a humidified chamber and incubated with protein blocking solution (5% normal horse serum and 1% normal goat serum in PBS) for 20 min at room temperature. The slides were incubated overnight at 4°C with primary antibody against α-SMA, CD31, Lyve-1 or desmin. Slides were then rinsed thrice with PBS and incubated for 10 min in protein blocking solution. For desmin staining, slides were incubated overnight at 4°C with Fab fragment goat anti-mouse IgG (Jackson ImmunoResearch Laboratories, West Grove, PA) to block endogenous immunoglobulins. This was followed by a short incubation with protein blocking solution and then by incubation with primary antibody. Slides were incubated for 1 hr at room temperature with Alexa 488-conjugated secondary antibody. Slides were then incubated overnight at 4°C with antibody against PDGF-Rβ or p-PDGF-Rβ. The sections were rinsed thrice with PBS and incubated for 10 min in protein blocking solution. Slides were incubated for 1 hr at room temperature with Alexa 546-conjugated goat anti-rabbit IgG secondary antibody. The samples were then rinsed thrice in PBS and nuclear counterstained with DAPI for 10 min. Samples were again rinsed thrice with PBS, and mounting medium was placed on each sample, which was protected with a glass coverslip. CAFs, endothelial cells or pericytes were identified by green fluorescence, whereas PDGF-Rβ or p-PDGF-Rβ was identified by red fluorescence.

Double immunofluorescence staining for CD31 (vascular endothelial cells) and desmin (pericytes)

To identify endothelial cells, slides were incubated overnight at 4°C with antibody against CD31. This was followed by incubation with Alexa 488-conjugated goat anti-rat IgG secondary antibody, and the slides were again blocked in a blocking solution as described above and incubated with antibody against desmin. After further washing and further blocking with blocking solution, the slides were incubated with Alexa 546-conjugated goat anti-rabbit IgG secondary antibody. Endothelial cells were identified by green fluorescence, whereas pericytes were identified by red fluorescence.

The coverage of pericytes on endothelial cells was determined by counting CD31-positive cells in direct contact with desmin-positive cells in five randomly selected microscopic fields (at 100× magnification).[31]

Immunohistochemical staining and terminal deoxynucleotide transferase-mediated dUTP-biotin nick end labeling (TUNEL)

Immunohistochemistry for α-SMA, Type-1 collagen, Ki-67 or Lyve-1 was performed on formalin-fixed, paraffin-embedded tissues cut into serial 4-μm sections. After deparaffinization and rehydration, tissue sections for staining of α-SMA, Type-1 collagen, Ki-67 or Lyve-1 were pretreated by microwaving them twice for 5 min in Dako REAL Target Retrieval Solution (Dako). Immunohistochemical staining for CD31 was done on fresh-frozen specimens cut into 8-μm sections. Frozen tissue sections were fixed in cold acetone for 10 min. Primary antibodies were applied to the slides and incubated overnight in humidified boxes at 4°C. After incubation for 1 hr at room temperature with corresponding peroxidase-conjugated secondary antibodies, a positive reaction was detected by exposure to stable 3,3′-diaminobenzidine for 5–10 min. Slides were counterstained with hematoxylin for visualization of the nucleus. Apoptotic cells in tissue sections were detected by TUNEL assay with the ApopTag Plus Peroxidase *In Situ* Apoptosis Detection Kit (CHEMICON, Temecula, CA) according to the manufacturer's instructions.

Quantification of the CAF (α-SMA-positive), collagen (Type-1 collagen-positive), microvessel (CD31-positive) and lymphatic vessel (Lyve-1-positive) areas

To evaluate angiogenic and lymphangiogenic activity of the tumors, the respective areas of vascular and lymphatic microvessels were quantified. Ten random fields at 100× magnification were captured for each tumor, and the outline of each vascular or lymphatic microvessel including a lumen was manually traced. The areas were then calculated with the use of NIH ImageJ software (Wayne Rasband, Bethesda, Maryland). The areas of CAF and extracellular matrix (ECM) were also determined from the respective areas of α-SMA-positive or Type-1 collagen-positive staining from 10 optical fields (100× magnification) of different sections.

Determination of the Ki-67 labeling index (Ki-67 LI) and the apoptotic index

The Ki-67 LI was determined by light microscopy at the site of the greatest number of Ki-67-positive cells. Cells were counted in 10 fields at 40× magnification, and the number of positive cells among ~ 1,000 tumor cells was counted and expressed as a percentage. The number of cells undergoing apoptosis was counted in five random 0.81-mm^2 fields at 100× magnification. The apoptotic index was taken as the ratio of positively stained tumor cells and bodies to all tumor cells and expressed as a percentage for each case.

Confocal microscopy

Confocal fluorescence images were collected by using a 20× or 40× objective lens on a Zeiss LSM laser scanning microscopy system (Carl Zeiss, Thornwood, NY) equipped with a motorized Axioplan microscope, argon laser (458/477/488/514 nm, 30 mW), HeNe laser (543 nm, 1 mW), HeNe laser (633 nm, 5 mW), LSM 510 control and image acquisition software and appropriate filters (Chroma Technology Corp., Brattleboro, VT). Confocal images were exported into Adobe Photoshop, and montages were prepared for publication photos.

Statistical analysis

Results are expressed as mean ± SE. Between-group differences in murine body weight, tumor weight and the areas of α-SMA-positive, Type-1 collagen-positive, CD31-positive and Lyve-1-positive cells were analyzed by Wilcoxon/Kruskal-Wallis test. Differences in the incidence of lymph node metastasis, liver metastasis and peritoneal metastasis were analyzed by Fischer's exact test. Differences in the percentages of Ki-67-positive cells and TUNEL-positive cells were analyzed by unpaired Student's *t*-test or χ^2 test as appropriate. A p value of <0.05 was considered statistically significant.

Results

Expression of PDGF-B and PDGF-Rβ in human gastric carcinoma cell lines

RT-PCR and Western blotting revealed that, under culture conditions, gastric carcinoma cells expressed PDGF-B mRNA, the level of which was higher in TMK-1 cells than in KKLS cells (Fig. 1*a*). PDGF-Rβ was expressed by MG63 cells but not by TMK-1 and KKLS cell lines (Figs. 1*a* and 1*b*). Phosphorylation of PDGF-Rβ in MG63 cells was inhibited by 1 μM imatinib (Fig. 1*c*).

Effect of imatinib on the growth of gastric carcinoma cell lines

To assess the effect of imatinib on growth of gastric carcinoma cell lines *in vitro*, cell proliferation assay was conducted. The reported clinically effective plasma concentration of imatinib is 1–5 μM.[32] Cell proliferation assay revealed no inhibition of gastric carcinoma cell growth after treatment with imatinib even when the concentration of imatinib was increased to 10 μM (Fig. 1*d*).

Expression of PDGF-B and PDGF-Rβ in human gastric carcinoma cells growing in the gastric wall of nude mice

In our orthotopic nude mouse models of KKLS and TMK-1 tumors, tumor cells were shown by immunofluorescence to express PDGF-B but not PDGF-Rβ. The expression level of PDGF-B protein was higher in TMK-1 cells than in KKLS cells (Figs. 2*a* and 2*e*). PDGF-Rβ immunoreactivity was predominant in the tumor stroma (Figs. 2*b* and 2*f*). Because the stroma of TMK-1 tumors expressed p-PDGF-Rβ (Fig. 2*g*), and it was more abundant than that of KKLS tumors (Figs. 2*d* and 2*h*), we used the TMK-1 cell line to identify which cell type in tumor stroma expresses PDGF-Rβ. We did this by double immunofluorescence staining for PDGF-Rβ and α-SMA (CAFs), CD31 (vascular endothelial cells),

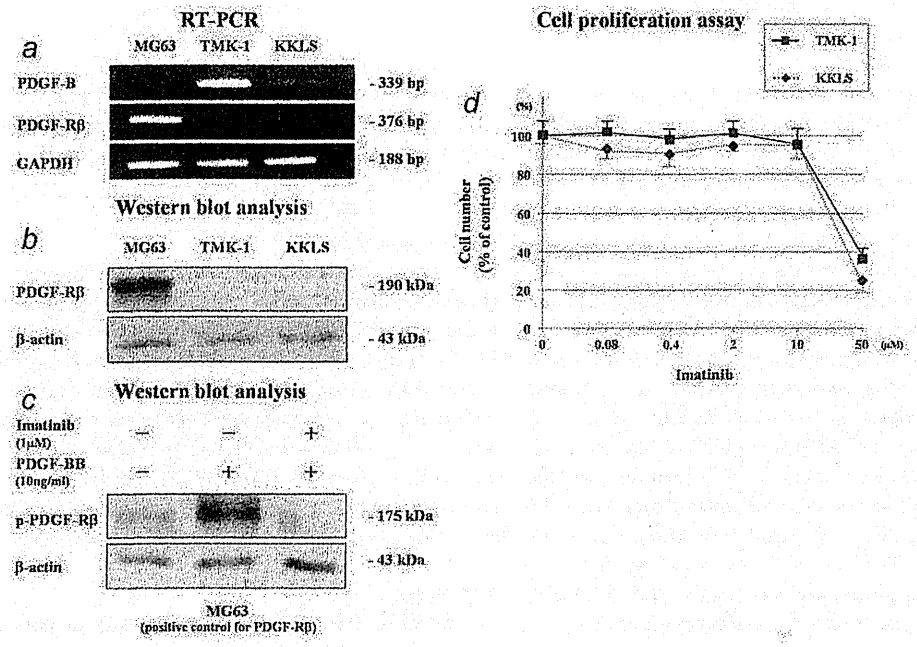

Figure 1. Reverse transcription polymerase chain reaction (RT-PCR) (*a*) and Western blot analysis (*b* and *c*) for expression of PDGF-B and PDGF-Rβ in gastric carcinoma cell lines. In MG63 cell line (positive control for PDGF-R expression), phosphorylation of PDGF-Rβ was inhibited by 1 μM imatinib (*c*). A dose-response curve for imatinib and the effect of growth inhibition *in vitro* in gastric carcinoma cell lines (*d*).

desmin (pericytes) or Lyve-1 (lymphatic endothelial cells). PDGF-Rβ protein co-localized with α-SMA protein, indicating CAFs expressed PDGF-Rβ (Fig. 2*i*). CD31-positive endothelial cells were covered by PDGF-Rβ-positive cells (Fig. 2*j*), which expressed desmin (Fig. 2*k*), indicating that pericytes expressed PDGF-Rβ. Lymphatic endothelial cells stained positively for Lyve-1. Lyve-1 protein also co-localized with PDGF-Rβ protein, suggesting that lymphatic endothelial cells expressed PDGF-Rβ (Fig. 2*l*).

Effect of imatinib on tumor stroma

When we examined the dose effect of imatinib on the inhibition of PDGF-Rβ phosphorylation in stromal cells, we found that the level of PDGF-Rβ expressed by CAFs in orthotopic TMK-1 tumors did not change with treatment (Fig. 3*a*). In contrast, phosphorylation of PDGF-Rβ was markedly inhibited in tumors of mice treated with high-dose imatinib (Fig. 3*b*). The stromal reaction in tumors was evaluated as the area of α-SMA-positive or Type-1 collagen-positive lesions. The effects of imatinib treatment on pericyte coverage of tumor-associated endothelial cells were evaluated by double immunofluorescence staining with anti-CD31 antibody and anti-desmin antibody. We noted morphologic differences between pericytes in the control group and pericytes in the imatinib treatment groups. Pericytes in the control group were enlarged and overlapped each other, whereas pericytes treated with imatinib were very thin (Fig. 3*c*). The stromal reaction was significantly reduced in mice treated with imatinib in comparison to that in control group mice (Figs. 4*a* and 4*b*). These effects were more remarkable in the high-dose imatinib treatment group than in the low-dose imatinib treatment group (Fig. 4*a*).

We also evaluated the dose effect of imatinib on tumor-associated microvessels. The vascular microvessel area (CD31-positive area) was significantly reduced in mice treated with imatinib in comparison with that in control group mice. This effect did not differ significantly between the low-dose and high-dose imatinib treatment groups (Fig. 4*c*). A decrease in the lymphatic vessel area (Lyve-1-positive area) was observed only in the group of mice treated with high-dose imatinib (Fig. 4*d*).

Treatment of human gastric carcinoma growing in the gastric wall of nude mice

We next determined the effects of imatinib, irinotecan and imatinib and irinotecan in combination on the growth and metastasis of TMK-1 human gastric carcinoma cells implanted in the gastric wall of nude mice. The tumor incidence was 100% in all treatment groups. Toxicity of the various treatment regimens was assessed on the basis of change in body weight. Oral administration of imatinib, intraperitoneal injection of irinotecan and administration of the two drugs in

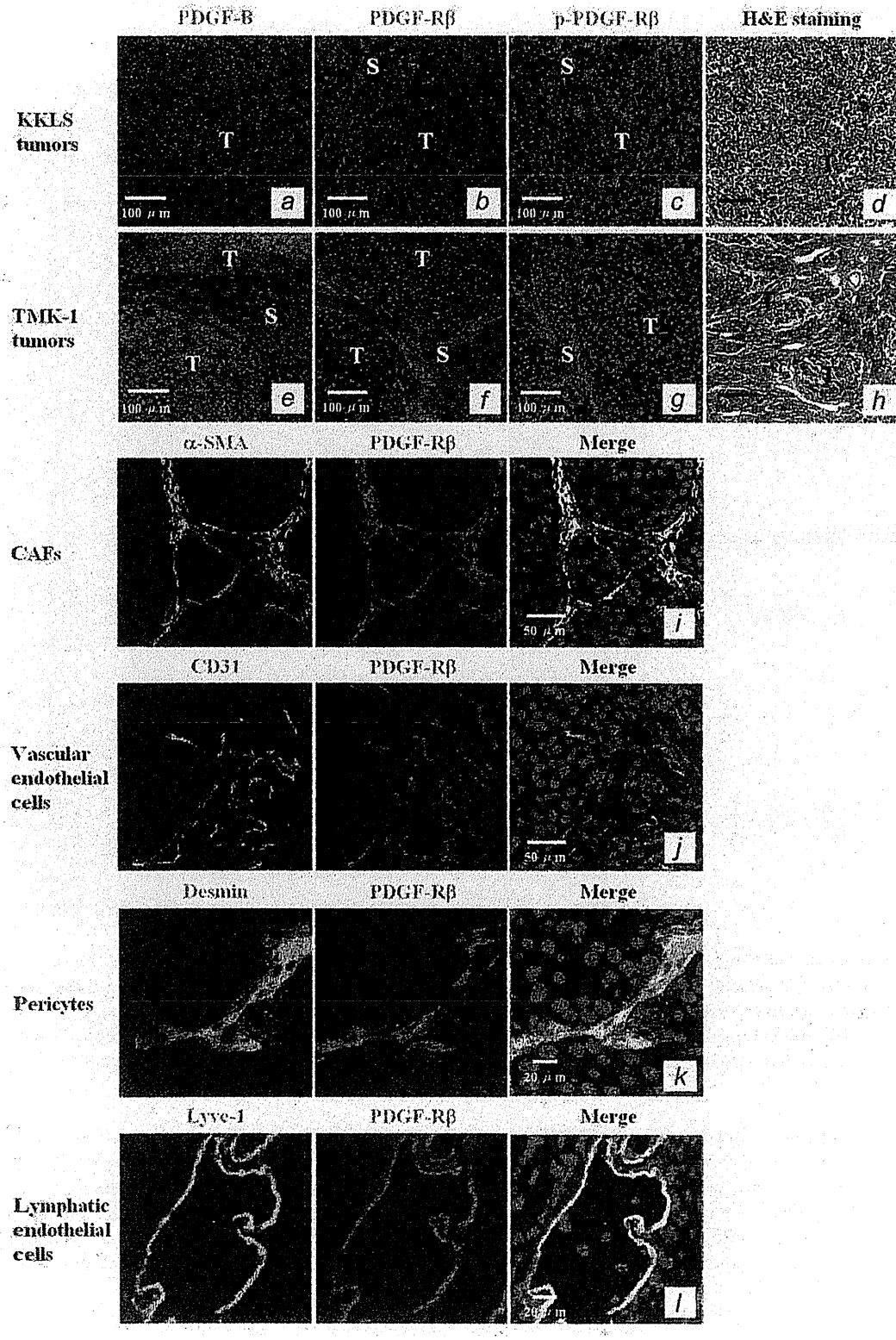

Figure 2. Hematoxylin and eosin (H&E) and immunofluorescence staining for PDGF-BB, PDGF-Rβ and p-PDGF-Rβ in KKLS and TMK-1 gastric carcinoma cells (*a–h*). Tumor cells stained positively for PDGF-B (*a* and *e*), whereas stromal cells stained positively for PDGF-Rβ (*b* and *f*). PDGF-Rβ was phosphorylated in TMK-1 tumors, but not in KKLS tumors (*c* and *g*) (red fluorescence). T, tumor nest; S, stroma. Double immunofluorescence staining for PDGF-Rβ and α-SMA (*i*), CD31 (*j*), desmin (*k*) and Lyve-1 (*l*). PDGF-Rβ-positive cells displayed red fluorescence, and α-SMA-, CD31-, desmin- and Lyve-1-positive cells displayed green fluorescence. Co-localization cells yielded yellow images.

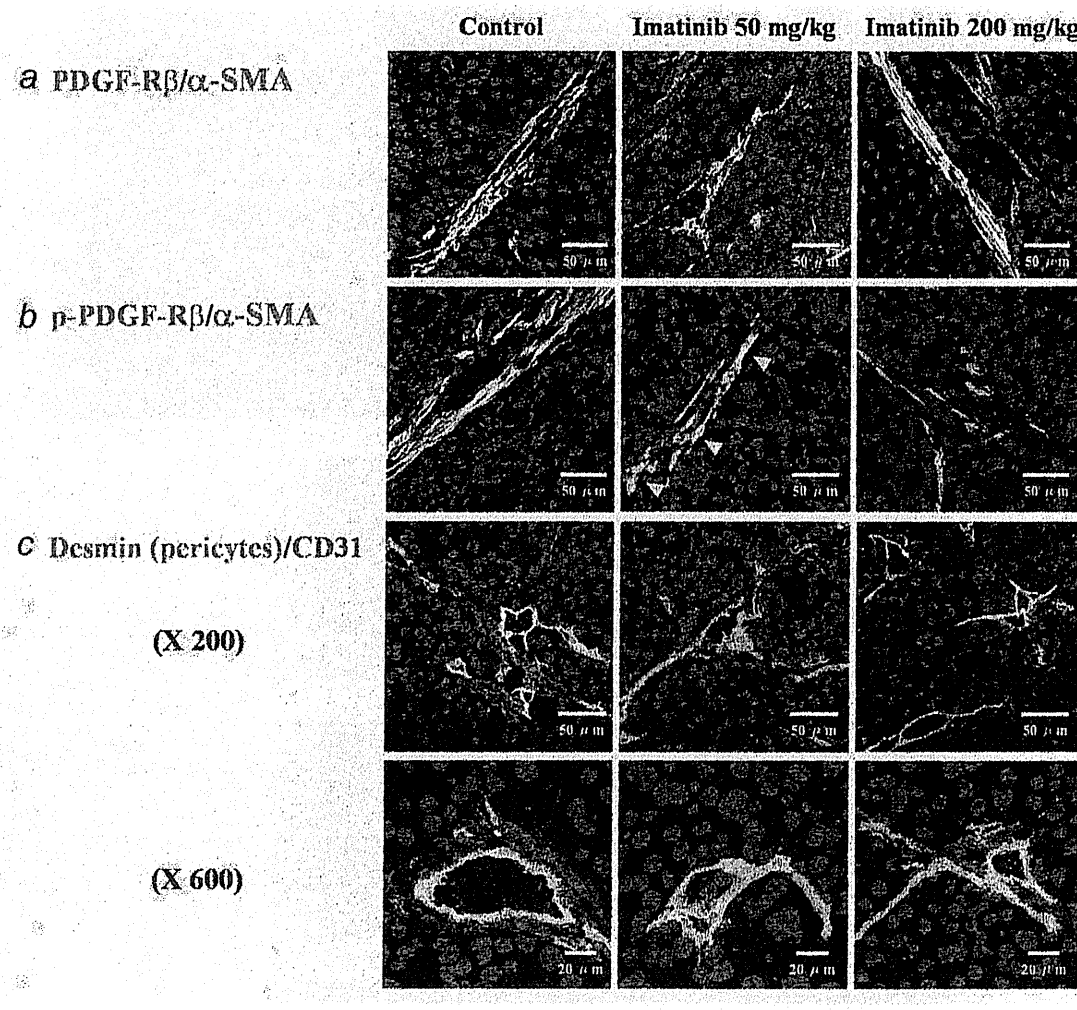

Figure 3. Effects of imatinib on carcinoma-associated fibroblasts (CAFs) and pericytes. Expression of PDGF-Rβ in CAFs did not change with treatment (*a*). Phosphorylation of PDGF-Rβ in CAFs was inhibited by treatment with imatinib. With low-dose (50 mg/kg/day) imatinib treatment, p-PDGF-Rβ expression was not completely inhibited (yellow arrowhead), but the inhibition was marked with high-dose (200 mg/kg/day) imatinib treatment (*b*). Endothelial cells were identified by green fluorescence, whereas pericytes were identified by red fluorescence (*c*). Morphological findings and the distribution of pericytes differed between control and imatinib treatment groups.

combination did not significantly affect body weights (Table 1). Tumor growth and metastasis were not inhibited in mice treated with imatinib alone (*vs.* control mice); however, tumor growth was significantly inhibited in mice treated with irinotecan alone or irinotecan combined with imatinib. Mice treated with high-dose imatinib and irinotecan in combination also had significantly smaller tumors than those in mice treated with irinotecan alone (Fig. 5*a*) or with low-dose imatinib in combination with irinotecan. Lymph node and peritoneal metastasis were inhibited only in the mice treated with high-dose imatinib and irinotecan in combination (Table 1).

For comparison, we evaluated the effects of imatinib on the growth of KKLS orthotopic tumors, for which the stromal reaction is minimal, with its effects on stromal compartment-rich TMK-1 tumors. Tumor growth was not inhibited in mice treated with imatinib alone. Although tumor growth was significantly inhibited in mice treated with irinotecan alone, high-dose imatinib used in combination with irinotecan did not enhance the antitumor effects of irinotecan (Fig. 5*b*).

Histopathologic analysis of TMK-1 tumors

In control and irinotecan-treated mice, TMK-1 gastric tumors showed abundant CAFs and ECM containing Type-1 collagen. In contrast, gastric tumors in mice treated with imatinib alone or with imatinib and irinotecan in combination were

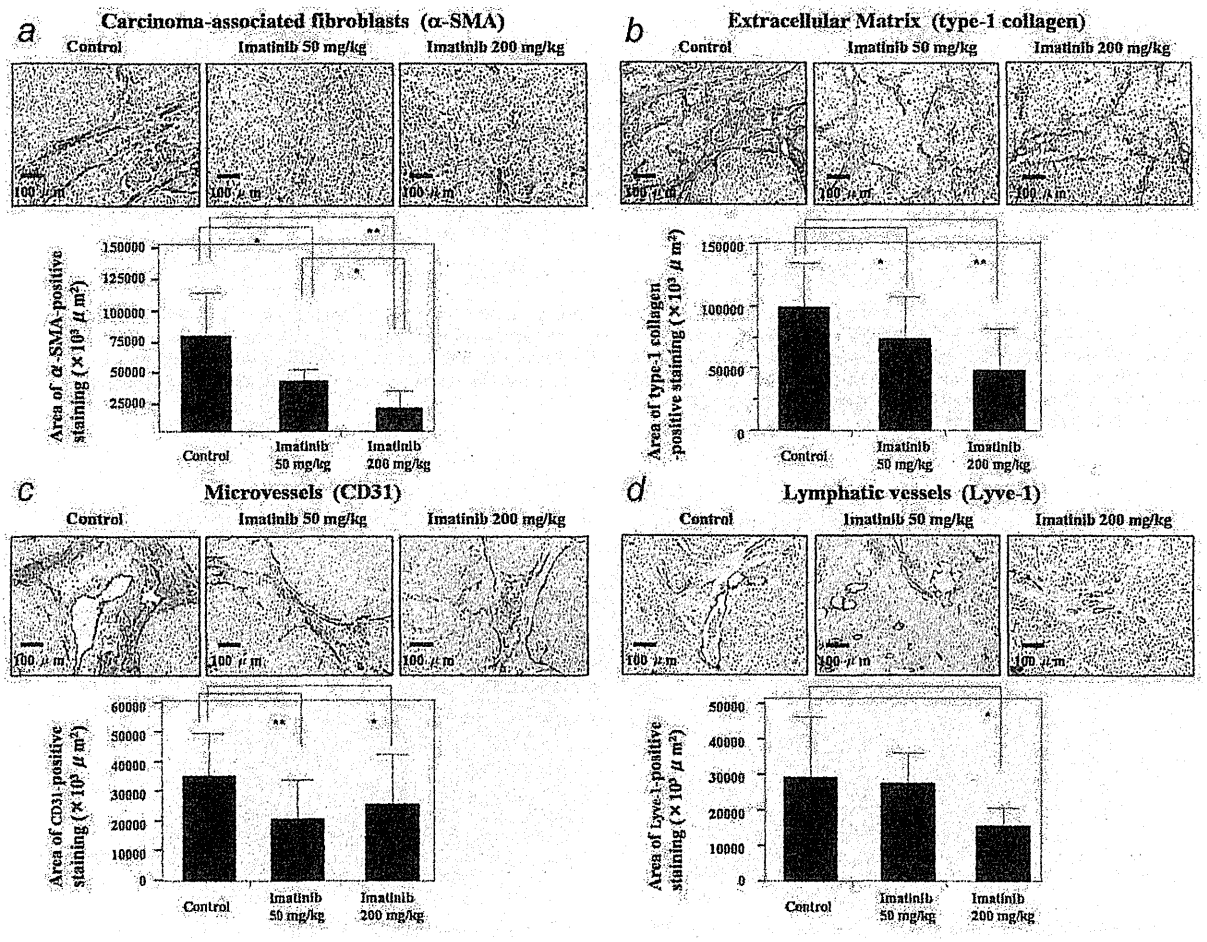

Figure 4. Dose-effects of imatinib on CAFs, extracellular matrix (ECM), vascular microvessels and lymphatic vessels were evaluated immunohistochemically according to the area of α-SMA (*a*), Type-1 collagen (*b*), CD31-positive (*c*) and Lyve-1-positive (*d*) cells, respectively. The areas of CAFs, ECM and vascular microvessels were reduced by treatment with imatinib. A reduction in the lymphatic area was observed only with high-dose imatinib treatment. *, $p < 0.05$, **, $p < 0.01$; bars, SE. [Color figure can be viewed in the online issue, which is available at wileyonlinelibrary.com.]

surrounded by scanty stroma (area of α-SMA-positive or Type-1 collagen-positive staining) (Fig. 6).

In addition, treatment with imatinib alone or with imatinib and irinotecan in combination significantly reduced the areas of vascular microvessels and lymphatic vessels as well as the number of pericytes (Table 2).

Proliferation of tumor cells was evaluated by staining for Ki-67. The control group Ki-67 LI was 57.3 ± 15.0. As shown in Table 2, the Ki-67 LI was significantly decreased after treatment with high-dose imatinib alone (41.7 ± 6.74, $p < 0.05$) or with irinotecan alone (37.7 ± 21.1, $p < 0.05$) and also after treatment with the two drugs in combination (39.7 ± 7.85; $p < 0.01$, 28.1 ± 14.3; $p < 0.01$, respectively).

According to TUNEL assay, the median number of apoptotic tumor cells in control mice was 5.54 ± 1.64. The number of apoptotic cells in tumors of mice from each of the treatment groups did not differ significantly from the number in control mice (Table 2).

Discussion

In our orthotopic nude mouse model of human gastric carcinoma, we found that blockade of PDGF-Rβ signaling by oral administration of PDGF-R tyrosine kinase inhibitor imatinib combined with intraperitoneal injection of irinotecan significantly inhibited not only the growth of tumors but also the incidences of lymph node and peritoneal metastasis. PDGF production and autocrine stimulation of cancer growth are described for only a subset of cancer types, *e.g.*, glioblastomas and sarcomas.[33,34] Most cancer cells, as secreting PDGF ligands, do not express PDGF-Rs, suggesting that PDGF may act as a paracrine growth factor.[35,36] In our experiments, PDGF-B was expressed by TMK-1 gastric carcinoma cells, whereas PDGF-